SiGe nanowires: Structural stability, quantum confinement, and electronic properties

Michele Amato,[1] Maurizia Palummo,[2] and Stefano Ossicini[3,*]
[1]*CNR-INFM-S3 "nanoStructures and bioSystems at Surfaces" and Dipartimento di Fisica, Università di Modena e Reggio Emilia, Via Campi 213/A, 41125 Modena, Italy*
[2]*European Theoretical Spectroscopy Facility (ETSF), CNR-INFM-SMC, Dipartimento di Fisica, Università di Roma "Tor Vergata," Via della Ricerca Scientifica 1, 00133 Roma, Italy*
[3]*CNR-INFM-S3 "nanoStructures and bioSystems at Surfaces" and Dipartimento di Scienze e Metodi dell'Ingegneria, Università di Modena e Reggio Emilia, Via Amendola 2 Pad. Morselli, I-42100 Reggio Emilia, Italy*
(Received 8 October 2009; revised manuscript received 19 November 2009; published 29 December 2009)

We report *first-principles* calculations of [110] SiGe NWs; we discuss the effect of geometry and composition on their thermodynamic stability, on their electronic properties, and on the nature of the quantum confinement effect. The analysis of formation enthalpy reveals that Ge_{core}/Si_{shell} NWs represent the most stable structure at any diameter, as a confirmation of the results of many experimental works. The study of the dependence of the energy band gap on the composition and geometry shows how *abrupt* NWs (wires with a clear flat interface between Si and Ge) present strongly reduced quantum confinement effect and offer a very easy way to predict and to engine energy band gap, which can have a strong relevance from a technological point of view. A careful analysis of the influence of composition on the wave-function localization and quantum confinement effect is also presented, in particular, for *core-shell* NWs.

DOI: 10.1103/PhysRevB.80.235333 PACS number(s): 73.22.−f, 71.15.Mb, 73.21.Hb

I. INTRODUCTION

Semiconductor nanowires (NWs) (Refs. 1–3) are one-dimensional nanostructures, which are opening substantial opportunities for the development of new electronic and optoelectronic devices that can overcome Moore's law limits.[4–6] Several studies have demonstrated the importance of these systems for applied physics, using them as electronic,[7] photovoltaic,[8–11] optoelectronic,[12,13] thermoelectric,[14] and low-temperature quantum devices.[15,16] A particular role in this research field is occupied by silicon-germanium (SiGe) NWs. In recent years, various methods of synthesis have been developed,[17–20] which guarantee a precise control of composition, morphology, and electronic properties. Several theoretical[21–25] and experimental[5,12,26,27] studies have shown that the electronic, transport, and optical properties of SiGe NWs, like other nanostructures, are strictly related to their low dimensionality and to the quantum confinement effect (QCE).[28–30] Moreover, they offer, unlike the corresponding pure single material NWs, the possibility of modulating band structure, band gap, and optical spectra by changing not only the size of the material but even the composition and the geometry of the system.[23,24,31] The interaction between Si and Ge atoms leads to a QCE that is very different from that one of the pure NWs and the band offset between the two different materials creates a spatial localization of electrons and holes,[21,25,31] which can remarkably modify transport and optical properties and that can be very useful for photovoltaics. In our recent work,[31] we have investigated the stability, the QCE, and the electronic properties of SiGe NWs, focusing in particular about the role of the geometry of interface Si/Ge on the formation enthalpy (FE) and on the electronic properties of the wires. We have demonstrated that the wires with a clear interface between Si and Ge regions, with the same number of Si and Ge atoms in the unit cell, (we called these systems half SiGe NWs; see Ref. 31 for more details) not only form the most stable structure but also show a strongly reduced quantum confinement effect (RQCE) with respect to the QCE of pure wires at the same diameter. Here, using first-principles calculations, we continue that type of analysis going into more depth the study of the SiGe wires presented in Ref. 31 and comparing them with core-shell SiGe NWs, which are attracting a lot of attention for their technological applications.[5] The methods and the models applied for SiGe NWs are described in Sec. II; the results concerning the structural stability and formation enthalpy are presented in Sec. III; in Sec. IV, we present the electronic properties of the wires, in particular, their dependence on the diameter and on the composition. In Sec. V, we sum up to conclusions.

II. METHODS

We have studied free-standing NWs with an approximately cylindrical shape and oriented along the [110] direction. The choice of this type of direction is induced by the experimental and thermodynamic observation that [110] crystallographic orientation represents the most preferred direction of wire growth at diameter smaller than 10 nm.[32] The diameter of the wires ranges from 0.8 to 1.6 nm and his definition is pointed out in Fig. 1. All the details of the geometrical construction of these nanostructures are the same in Refs. 29–31. The NWs surface has been passivated with hydrogen atoms in order to eliminate the surface states from the fundamental energy-band-gap range. Figure 1 shows the top views of all the different types of NWs we have analyzed: pure Ge and Si NWs are shown in Figs. 1(a) and 1(b). The other four structures are different types of SiGe NWs: the first one is an example of random SiGe NWs (*random* NWs), where the distribution of the two types of atoms in the unit cell is completely random[33,34] [see Fig. 1(c)]; the second one is abrupt SiGe NWs (*abrupt* NWs), in which there is a planar

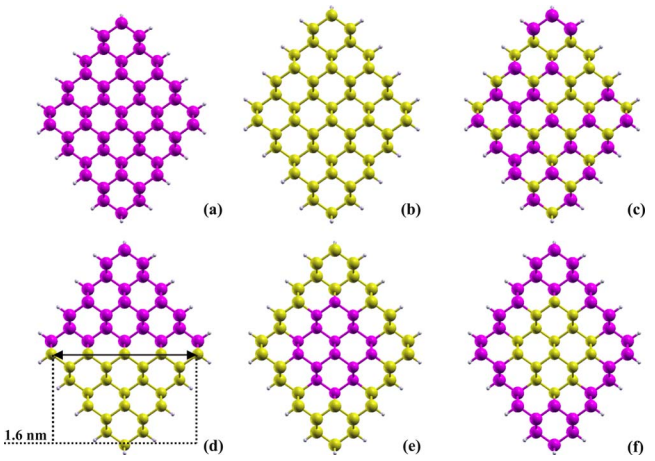

FIG. 1. (Color online) Top view of Ge (a), Si (b), and SiGe random (c), abrupt (d), Ge_{core}/Si_{shell} (e), Si_{core}/Ge_{shell} and (f) nanowires with a diameter $d=1.6$ nm. Yellow/light gray spheres represent Si atoms, magenta/dark gray spheres Ge atoms, while the small white spheres are H atoms used to saturate the dangling bonds.

Si/Ge interface along the shortest dimension of the transverse cross section of the wire [see Fig. 1(d)] (it is important to note that the half SiGe NWs of Ref. 31 are a particular type of *abrupt* NWs with a fixed composition of silicon $x_{Si}=0.5$ and germanium $x_{Ge}=0.5$). The two last types represent core-shell SiGe NWs (*core-shell* NWs), radial heterostructures, which are made by two coaxial cylinders: the internal one (the *core*) is made up by a type of atom and the external one (the *shell*) made up of the other type of atom.[17] Figure 1(e) shows Ge_{core}/Si_{shell} NWs, while Fig. 1(f) Si_{core}/Ge_{shell} NWs. For all SiGe NWs, the compositional range is $0 \leq x \leq 1$, where x is the relative composition of one type of atom with respect to the total number of atoms in the unit cell (all the functions of the composition presented in the text can be easily read as a function of x_{Si} or x_{Ge} by making a change in variable because the two variables are related by the relation $x_{Si}+x_{Ge}=1$).

We performed *ab initio* calculations within the single-particle density-functional theory in the local-density approximation (DFT-LDA),[35–38] as implemented in the QUANTUM ESPRESSO package;[39] norm-conserving pseudopotentials have been used. The supercell is taken to be large enough (more than 10 Å of vacuum) orthogonal to the growth direction to eliminate the interaction between neighbor wires. An energy cutoff to 30 Ry and a grid of $16\times1\times1$ points for the sampling of the Brillouin zone have been used. The mismatch between the lattice parameter of the silicon and germanium bulk is nearly 4%; then, for the SiGe NWs, it is important to take into account the effect of the strain between the two different materials. We performed for all the considered NWs a full geometry optimization through the Broyden-Fletcher-Goldfarb-Shanno technique; thus, regarding the positions of the Si and Ge atoms in the plane normal to the growth direction of the wires, these positions fully take into account strain effects. Concerning the growth direction of the wire, the strain has been considered in different ways by choosing different translational periodicity depending on the type of the wire (for [110] SiGe NWs the translational periodicity is $\frac{a_{bulk}}{\sqrt{2}}$, where a_{bulk} is the optimized lattice parameter of the bulk[40]). For pure Si and pure Ge NWs, we choose $a_{Si}=5.40$ Å (corresponding to pure Si bulk), $a_{Ge}=5.59$ (corresponding to pure Ge bulk); for random, abrupt, and core-shell SiGe NWs, we choose the lattice parameter derived from Vegard's law for semiconductor bulk alloys,[41] which states that the relaxed lattice parameter of a two component system is a linear function of the composition. In the case of *random* NWs, this choice is supported by the experimental results of Refs. 12 and 42; while for *core-shell* NWs several theoretical studies[24,25] have demonstrated that these systems roughly follow the Vegard's law.[43,44] Nevertheless, we have carefully checked the effect of different lattice parameters (pure Si, pure Ge, and Vegard's law) on the stability and electronic properties of all the types of SiGe NWs and we can say that the electronic band-gap and the wave-function localizations are really independent from the choice of the lattice parameter in the growth direction and are related only to the geometry relaxation in its normal plane. Moreover, the variations in formation energies values as a consequence of the choice of the different translational periodicity are very small and do not change the obtained physical results. The input Ge-H bond length is 0.1525 nm and the input Si-H bond length is 0.1480, corresponding to that of the GeH_4 molecule and of SiH_4 molecule, respectively. All the properties presented in the text are referred to the optimized geometries.

III. STRUCTURAL STABILITY AND FORMATION ENTHALPY

The calculation of the FE of nanostructures is a very useful tool to understand and predict the thermodynamic properties of unknown systems[45–51] and can give crucial information to experimentalists for the synthesis of these kinds of materials. In our previous work,[31] we have reported some calculations of FE for *abrupt* (*half*), *random*, and *mixed* NWs (with fixed composition $x_{Si}=0.5$ and $x_{Ge}=0.5$), analyzing its dependence on the atomic configuration in the unit cell and on the wire's diameter and showing how *abrupt* NWs (*half*) represent the most stable SiGe NWs and their stability is more pronounced increasing the diameter; moreover, on the basis of that results we concluded that at zero temperature, the segregation is favored with respect to mixing (this statement is in agreement with theoretical and experimental results about SiGe superlattices[52–54]). Here we follow that analysis, presenting calculations of FE for *core-shell* NWs, analyzing its dependence on diameter and composition and comparing them with results for pure, *abrupt*, and *random* NWs. For core-shell geometry, the variation in composition is obtained increasing gradually the size of the core and fixing the diameter, as shown in Fig. 2.

As in Ref. 31, the FE has been evaluated, following the way proposed by Ferrando *et al.*[55] for metallic nanoalloys:

$$\Phi^*(Si_nGe_mH_l) = E_{tot}(Si_nGe_mH_l) - m\frac{E_{tot}(Ge_NH_l)}{N} - n\frac{E_{tot}(Si_NH_l)}{N}, \quad (1)$$

where E_{tot} is the ground-state total energy of a given SiGe

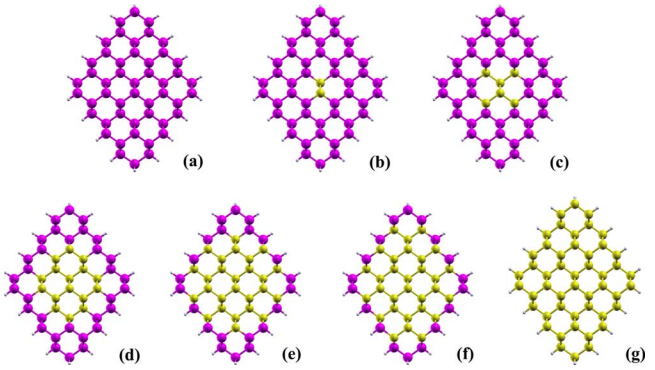

FIG. 2. (Color online) Top view of Si_{core}/Ge_{shell} NWs with diameter 1.6 nm and with composition x_{Si} equal to 0 (a), 0.042 (b), 0.125 (c), 0.333 (d), 0.542 (e), 0.625 (f), and 1 (g). The same geometrical configurations are used to analyze the composition dependence of Ge_{core}/Si_{shell} (one has only to invert color of Si and Ge). Yellow/light gray spheres represent Si atoms, magenta/dark gray spheres Ge atoms, while the small white spheres are H atoms used to saturate the dangling bonds.

NW and $N=n+m$. In Eq. (1), we are subtracting from the binary nanoalloy the appropriate fraction of the configurational energy of pure reference Si and Ge NWs; in this way, Φ^* is an unbiased quantity being zero for pure NWs. The most stable configuration is characterized by the lowest value of Φ^*. It is important to point out that this equation is applied assuming zero pressure and neglecting the vibrational contribution and the zero-point energy.[56–58] The trend of FE as a function of composition for *core-shell* NWs at different diameter is shown in Fig. 3.

Observing the figure, it is clear that we have different results depending on the material that constitutes the core: in particular, we can say that for Si_{core}/Ge_{shell} the FE is always positive, indicating instability with respect to the pure NWs [which have, following Eq. (1), FE equal to zero]. This instability is more pronounced increasing the diameter. Ge_{core}/Si_{shell} has negative values of FE, indicating more stability with respect to the pure wires and to the Si_{core}/Ge_{shell}. This means that, for this kind of geometry, Ge atoms tend to occupy the *core* of the wire, lowering the FE of the system. Although the technological success of *core-shell* NWs, any report on the theoretical characterization of their FE is not available, to the best of our knowledge, up to now. For this reason, we cannot compare our results with other theoretical studies about FE of SiGe NWs. Nevertheless, our results are in qualitative agreement with those presented by Ramos *et al.*[59] about SiGe nanocrystals and by a lot of theoretical and experimental observations about other SiGe systems,[60–66] where the most common structures are Ge_{core}/Si_{shell} nanostructures. (The size of the experimental SiGe systems is one order of magnitude bigger than the size of our wires; so the comparison has to be considered only as a qualitative one. We only want to point out that our results can show a thermodynamic property that has been already demonstrated for other SiGe systems.) Finally, from our calculations, we can extract a trend of the FE for *abrupt*, *random* (presented in Ref. 31), and *core-shell* NWs. All the wires have $d=1.6$ nm and composition x_{Ge} nearly 0.5. The trend of FE is the following:

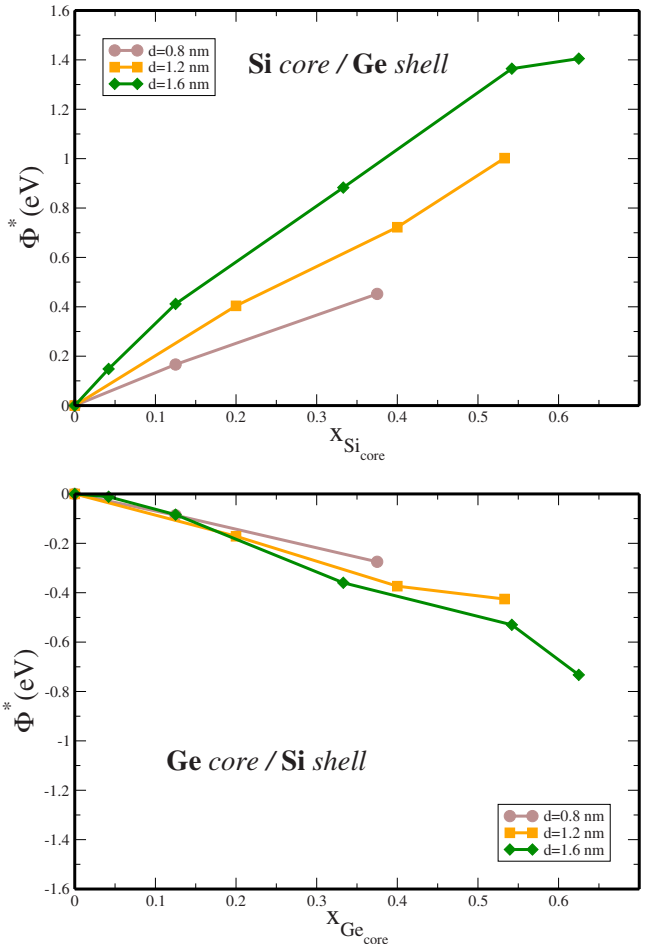

FIG. 3. (Color online) Formation enthalpy for Si_{core}/Ge_{shell} (top panel) and Ge_{core}/Si_{shell} (bottom panel) as a function of composition and for different diameters. The same quantity for the corresponding pure Si and Ge NWs is zero at any diameter for Eq. (1).

$$\Phi^*(Si_{core}/Ge_{shell}) > \Phi^*(\text{random}) > \Phi^*(\text{abrupt}) > \Phi^*(Ge_{core}/Si_{shell}). \quad (2)$$

The most stable structures are Ge_{core}/Si_{shell} NWs, which have negative values of FE and for which we can say that, in general, the creation of a nanoalloy with this geometry is favored. All the other structures have positive values of FE, so for these NWs we can say that the mixing is unfavorable with respect to the pure wires. The least-favored configuration is the Si_{core}/Ge_{shell}, while *abrupt* and *random* NWs are intermediate between the two core-shell geometries.

IV. ELECTRONIC PROPERTIES

For [110] pure Si and pure Ge NWs, it has been demonstrated that the energy band gap (E_g) decreases monotonically with the wire's diameter[28–30,37,67] as a clear consequence of the reduction in the size of the system and related QCE. Other studies on SiGe NWs (Refs. 22–25 and 31) have shown how the QCE in these type of wires can be very reduced with respect to the pure ones (RQCE) depends strongly on the geometry and on the composition of the sys-

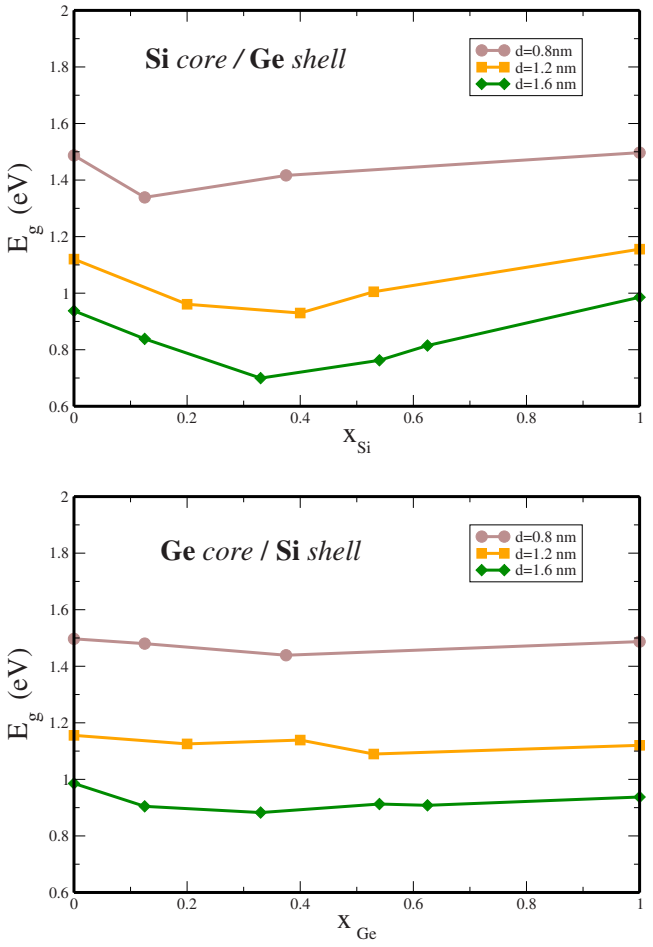

FIG. 4. (Color online) DFT-LDA electronic gaps E_g as a function of Ge composition (Si composition) for $Ge_{core}/Si_{shell}(Si_{core}/Ge_{shell})$; x_{Ge} and x_{Si} are the relative composition of one type of atom with respect for the total number of atoms in the unit cell.

tem and can be affected by the band offset between Si and Ge. In particular, for SiGe NWs, as clearly explained by Yang *et al.*,[12] the QCE depends principally by two main effects: one is the *intrinsic* bulk alloying effect, which is related to the composition of the system and the geometry of interface between Si and Ge; the other one is an *extrinsic* size effect and is related to the reduction in the size of the system. Both the effects have a primary role in the definition of the QCE for SiGe heterostructures and an analysis of their different physical nature can be interesting. In Ref. 31, we have found that in some types of SiGe NWs, when the size is reduced, the opening of the bulk band gap due the QCE is quite attenuate with respect to that of pure Si and Ge wires. In particular, analyzing the effect of the reduction in the size for some SiGe NWs with fixed composition, we have shown how, for *abrupt* NWs (*half*), increasing the diameter the RQCE is more pronounced. In the following, we analyze how the variation in the composition on different geometries affects E_g and the spatial localization of the wave function, modifying in different ways the QCE. To achieve this goal, we have divided this section into two parts: in the first one, we report the scaling of E_g with composition x for all the

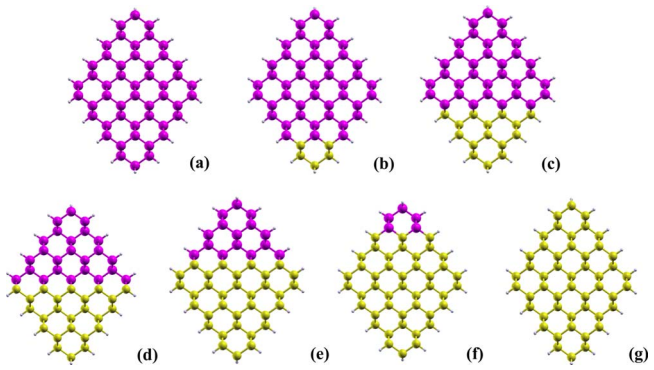

FIG. 5. (Color online) Top views of *abrupt* NWs with diameter 1.6 nm and with composition x_{Ge} equal to 1 (a), 0.895 (b), 0.687 (c), 0.5 (d), 0.312 (e), 0.104 (f), and 0 (g). Yellow/light gray spheres represent Si atoms, magenta/dark gray spheres Ge atoms, while the small white spheres are H atoms used to saturate the dangling bonds.

geometries; in the second one, we try, through the plots of the wave-function localizations, to give a physical explanation of the $E_g(x)$ trends, pointing out the combined role of the geometry and of the composition for RQCE.

A. RQCE: Scaling of E_g with composition

Some theoretical[23,24] studies have demonstrated that for [111] *core-shell* NWs, the E_g is a nonlinear function of the composition, as a consequence of the opposite variation in core and shell sizes with composition x for a given nanowire with fixed diameter. In order to analyze the intrinsic bulk alloying effect on SiGe NWs, we have studied the effect of the variation in composition (at fixed diameter) for different geometries, in particular, for *core-shell*, *abrupt*, and *random* NWs. First we report in Fig. 4, the trend of electronic E_g (Ref. 68) as a function of the composition for Ge_{core}/Si_{shell} (bottom panel) and Si_{core}/Ge_{shell} (top panel) for $d=0.8$, 1.2, 1.6 nm.

The two figures clearly show a nonlinear dependence of the energy band gap on the composition of the wire, with observable minima $x\sim 0.2-0.4$. Further increase of x results to an increasing of the E_g, corresponding to the pure Si and Ge NWs (which have similar gaps). This finding reproduces qualitatively the results obtained by Musin and Wang[23] for [111] direction. In particular, it can be deduced that the QCE is more reduced when the *core* is made up of silicon than germanium since the decreasing of the energy band gap is major in Si_{core}/Ge_{shell} than in Ge_{core}/Si_{shell}. Finally, it is important to mention that the observed effect is more pronounced increasing the diameter. For *abrupt* NWs, the variation in composition is obtained by adding or deleting some rows of one type of atom in the transverse section (along the direction of the shortest dimension) of the wire in order to preserve a clear interface between Si and Ge (that is the main feature of this type of wire), as shown in Fig. 5. In Fig. 6, we report the scaling of DFT-LDA energy band gap with the Ge composition x_{Ge} for *abrupt* NWs with $d=1.6$ nm. The calculated values are fitted very well by a quadratic function of the composition, which is represented by the dotted orange

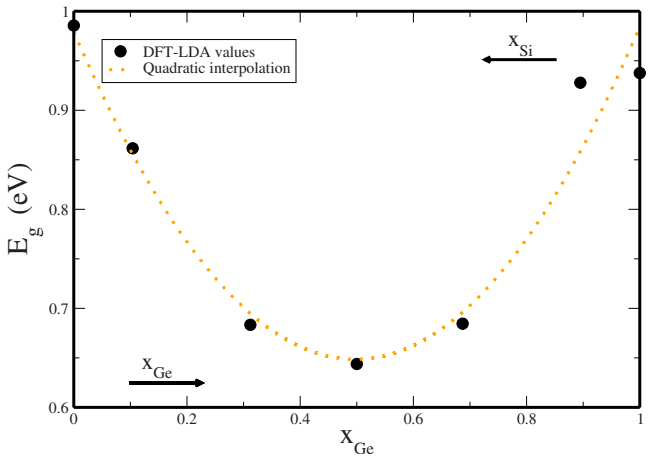

FIG. 6. (Color online) DFT-LDA electronic gaps E_g as a function of Ge composition x_{Ge} for *abrupt* NWs with $d=1.6$ nm (black circle) a quadratic interpolation of the data [corresponding to Eq. (3) is also shown (dotted orange line]. One can read the curve even as a function of Si composition x_{Si} (from right to left) obtaining Eq. (4).

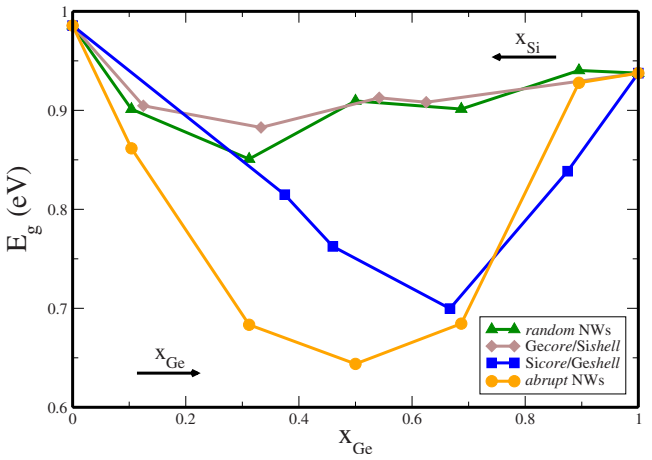

FIG. 7. (Color online) DFT-LDA electronic gaps E_g as a function of Ge composition x_{Ge} for random (green line), $\mathrm{Ge}_{core}/\mathrm{Si}_{shell}$ (brown line), $\mathrm{Si}_{core}/\mathrm{Ge}_{shell}$ (blue line), and *abrupt* (orange line) NWs with $d=1.6$ nm. One can read the curve even as a function of the Si composition x_{Si} (from right to left).

line and which have the following analytical form (in eV):

$$E_g(x_{\mathrm{Ge}}) = 0.98292 - 1.3508x_{\mathrm{Ge}} + 1.3478x_{\mathrm{Ge}}^2 \qquad (3)$$

or analogously can be expressed as a function of x_{Si} in the form

$$E_g(x_{\mathrm{Si}}) = 0.98292 - 1.3508x_{\mathrm{Si}} + 1.3478x_{\mathrm{Si}}^2. \qquad (4)$$

The scaling of the energy band gap for these type of wires is perfectly quadratic with the composition. This behavior is perfectly symmetrical if we add silicon or germanium to the system and is totally different from the behavior of core-shell systems (see Fig. 4). Moreover, as shown in Ref. 31, the QCE in this type of configuration is strongly reduced with respect to the pure wires as a consequence of the band offset between Si and Ge regions. This symmetrical property (in part due to the very similar E_g of the pure wires at these diameters) shows a very useful tool for the modulation of the energy band gap for this type of materials and could have relevant technological applications.

In Fig. 7, we report a comparison of the scaling of E_g with Ge composition x_{Ge}, for all the NWs we have studied (with $d=1.6$ nm): from the figure, it is clear that all the geometries present a decreasing in the energy band gap (RQCE) with respect to the pure wires by changing the composition of the system. This dependence has different analytical forms, depending on the geometry of the wire. Looking at the curve for *random* NWs, it is clear that even in this type of wires, where the distribution of the two types of atoms is completely random, it is possible to observe a RQCE, which is, as in the case of *core-shell* NWs, a nonlinear function of the composition. Moreover, the observed scaling of E_g with Ge composition x_{Ge} for *random* NWs is qualitatively in agreement with the experimental band-gap modulation measured by Yang *et al.*[12] for *random* NWs.[69]

B. RQCE: Wave-function localization

In the following, we present a careful analysis of the variation in the wave-function localization with the composition, in order to point out the origin of the differences in the electronic properties, discussed in the previous section.

As shown above, the most pronounced RQCE is present in *abrupt* NWs, for which the function $E_g(x_{\mathrm{Ge}})$ is parabolic and has a minimum at $x_{\mathrm{Ge}}=0.5$. The origin of this effect is related to the particular geometry of the system (a planar interface between Si and Ge) and to the different QCE of Si and Ge.[31] These factors induce a type II staggered band offset between Si and Ge, which implies that the valence-band maximum (VBM) is located on the germanium part of the wire, while the conduction-band minimum (CBM) is located on the silicon part and, moreover, it reduces the QCE with respect to the pure wires. In Fig. 8, we report the variation in the VBM and CBM localizations with composition for *abrupt* NWs with $d=1.6$ nm. From the figure, it can be noted that the type II offset is preserved even varying the composition: in fact, for all the different values of x_{Ge}, the VBM is always located on Ge part of the wire, while the CBM on the Si part (so we can conclude that the composition has small influence on the shape and on the localization of the wave function). This fact means that for *abrupt* NWs, the geometry plays a crucial role. The type II band offset and consequent strong RQCE are present even with a very little variation in the composition but preserving a planar interface between silicon and germanium. A confirmation of the central role of the geometry for the RQCE for *abrupt* NWs stands out analyzing the trend of E_g for *random* NWs. As we have explained in Ref. 31, the spatial carrier localization and consequent type II offset are partially present in this type of NWs, depending on the size of the regions of Si or Ge that are present in the transverse section of the wire. From Fig. 7, it is clear that the dependence of E_g from the composition is weak, and the extent of the RQCE is small compared to that one found in *abrupt* NWs. This happens because in this kind

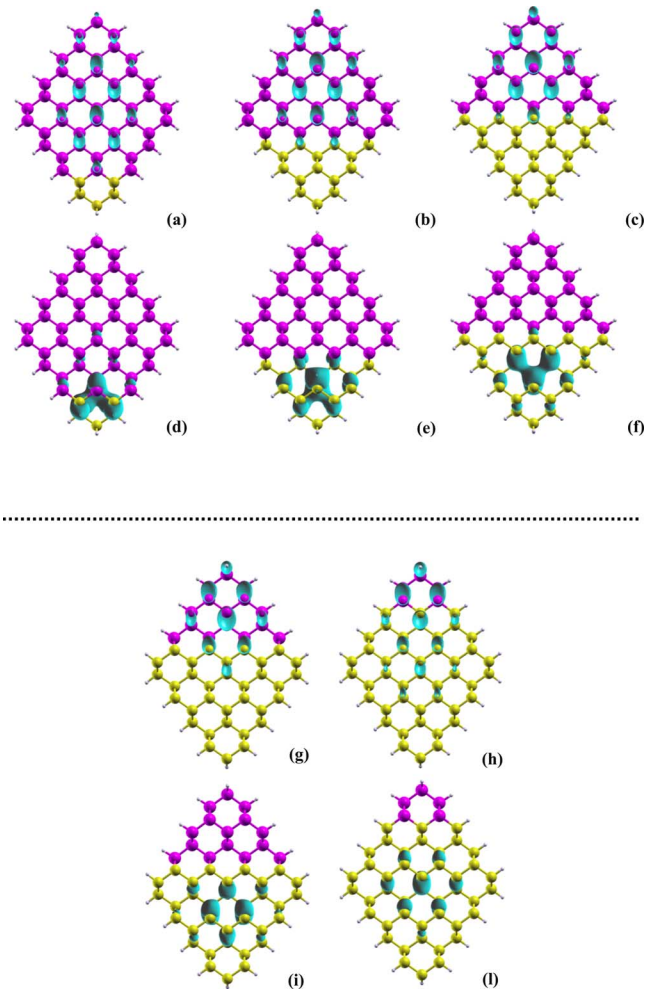

FIG. 8. (Color online) VBM (first and third rows) and CBM (second and fourth rows) wave-function localizations for *abrupt* NWs with diameter $d=1.6$ nm and composition x_{Ge} equal to 0.895 [(a) and (d)], 0.687 [(b) and (e)], 0.5 [(c) and (f)], 0.312 [(g) and (i)], and 0.104 [(h) and (l)]. Yellow/light gray spheres represent Si atoms, magenta/dark gray spheres Ge atoms, while the small white spheres are H atoms used to saturate the dangling bonds.

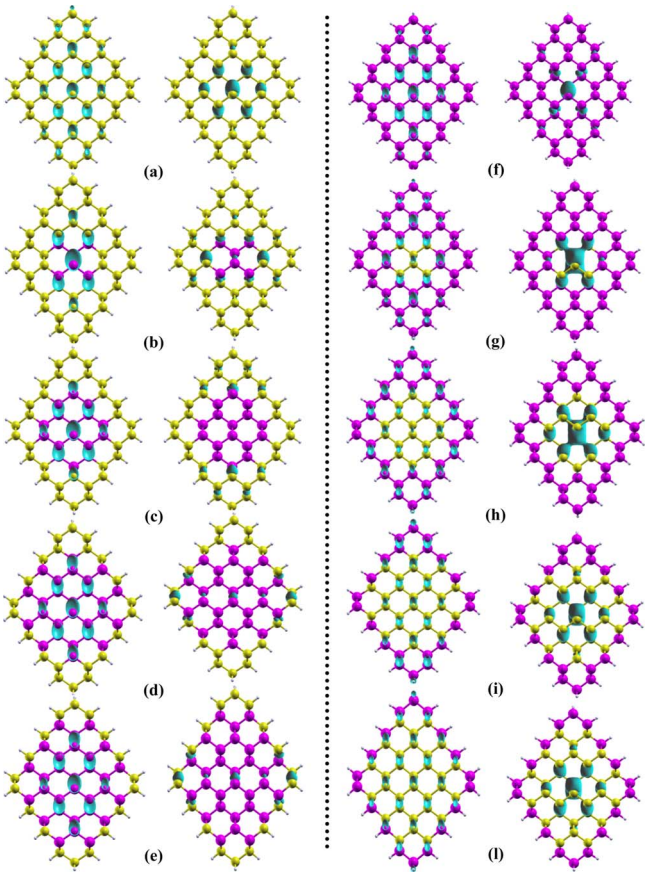

FIG. 9. (Color online) VBM (first and third columns) and CBM (second and fourth columns) for Ge_{core}/Si_{shell} NWs (left side) and Si_{core}/Ge_{shell} NWs (right side) with diameter $d=1.6$ nm and composition x_{Ge} (left side) and x_{Si} (right side) equal to 0 [(a) and (f)], 0.125 [(b) and (g)], 0.333 [(c) and (h)], 0.542 [(d) and (i)], and 0.625 [(e) and (l)]. Yellow/light gray spheres represent Si atoms, magenta/dark gray spheres Ge atoms, while the small white spheres are H atoms used to saturate the dangling bonds.

of wire, the geometry does not create the conditions for a type II band alignment. Then, for these two cases, we can say that to explain the nature of intrinsic bulk alloying effects, we must take into account both the composition and the geometry of the system. In fact, the same value of x_{Ge} in different wires induces different RQCE. Finally, the planar interface geometry between Si and Ge seems to be an essential requirement for the RQCE.

For core-shell geometry, the $E_g(x)$ is nonlinear, as a consequence of the opposite variation in *core* and *shell* sizes at composition x for a given nanowire with fixed diameter.[70] After *abrupt* NWs, the geometry that present a strong RQCE is Si_{core}/Ge_{shell} NWs, while for Ge_{core}/Si_{shell} NWs the reduction of E_g is less pronounced and more similar to that observed in *random* NWs. The origin of this different behavior between the two *core-shell* NWs is related to the variation in the distribution of the electronic states as the size of the core and the shell varies. The analysis of the band-gap scaling for *core-shell* NWs is quite complicated. In this type of NWs, in fact, Si and Ge states are confined in different ways depending on they constitute the shell or the core of the wire: shell and core may rise up to different QCE.[21,25] In other words, two different factors have to be considered: the first one is the fact that, as we have demonstrated in Ref. 31, Ge presents a stronger QCE than Si and that, while Si confines mainly in the valence states, the effect of QCE for Ge is similar for the valence and the conduction bands (for more details see Refs. 71–73); the second aspect to consider is related to the geometry of the system, in particular, to the fact that the interface between Si and Ge is a circular one and that *core* and *shell* induce different confinement.

To understand more deeply this point in Fig. 9, we report the wave-function localization for the electronic states of conduction- and valence-band edges: as one can see for Si_{core}/Ge_{shell} NWs (right side of Fig. 9), an increase in the core size strongly localizes the CBM in the core, while the VBM is rather delocalized in all the section of the wire and is much similar to that one of the pure Ge NWs. An analysis of the band structure for Si_{core}/Ge_{shell} NWs, in agreement with by other theoretical studies,[25] shows how the discretization of the states due to the QCE in the conduction band is more

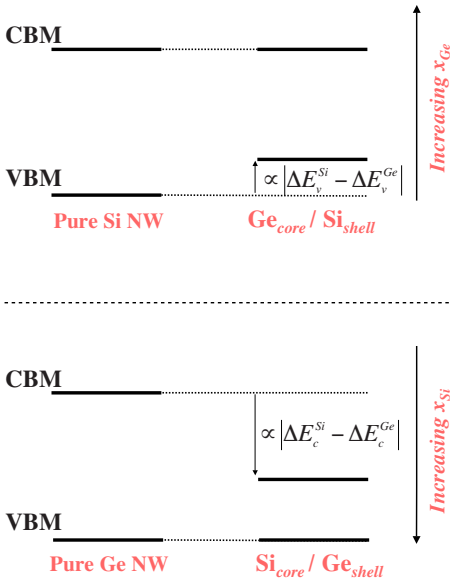

FIG. 10. (Color online) Qualitative model of for RQCE in *core-shell* NWs. The mechanism of the reduction in the energy band gap with respect to the pure NWs is shown in the upper panel for Ge_{core}/Si_{shell} NWs and in the bottom panel side for Si_{core}/Ge_{shell} NWs.

significant that the one for valence states. This means that germanium, which presents more pronounced QCE in conduction band than silicon ($\Delta E_c^{Ge} > \Delta E_c^{Si}$; see Ref. 73), shifts up his electronic states more than an increase in the core size silicon: this fact localizes the CBM of the Si_{core}/Ge_{shell} wire on the Si core (as shown in Fig. 9) and shifts down its value with respect to the CBM of the pure Ge NW. The valence band that presents a less significant discretization of states is less affected by the increasing of Si core and roughly conserves the value of VBM of the pure Ge NW (see Fig. 10). So these two combined effects induce a reduction of the E_g with respect to the pure Ge NW; the RQCE for these type of wires is stronger with respect to the one of Ge_{core}/Si_{shell} wires.

In fact for Ge_{core}/Si_{shell} (left side of Fig. 9), the increasing of the core size strongly localizes the VBM in the core and at the same time spreads the CBM (localized in the core for Si pure NW) into the silicon shell region of the wire;[24] an analysis of the band structure for Ge_{core}/Si_{shell} NWs, confirmed also by Ref. 25, shows how the discretization of the states due to the QCE in the valence band is more significant that the one for conduction states; this means that silicon, which presents more pronounced QCE in valence band than germanium ($\Delta E_v^{Si} > \Delta E_v^{Ge}$; see Ref. 73), shifts down his electronic states more than germanium: this fact localizes the VBM of the Ge_{core}/Si_{shell} wire on the Ge core, as shown in Fig. 9, and shifts up his value with respect to the VBM of the pure Si NW. The conduction band of the Ge_{core}/Si_{shell} wire that presents a less significant discretization of states is less affected by increasing of Ge core and is localized in the silicon shell, roughly conserving the value of CBM of the pure Si NW (see Fig. 10). The origin of the weak RQCE (with respect to the Si_{core}/Ge_{shell} case) for these wires is related to the fact that the differences of the extent of the shift of CBM for pure Si and pure Ge NWs are bigger than that of VBM ($|\Delta E_c^{Si} - \Delta E_c^{Ge}| \gg |\Delta E_v^{Si} - \Delta E_v^{Ge}|$; see Ref. 73), then in the first case Si_{core}/Ge_{shell} a more pronounced RQCE than the one observed in Ge_{core}/Si_{shell} is obtained (this model of alignment of VBM and CBM is reported in the scheme of Fig. 10).

Thus, for *core-shell* NWs, we can say that the scaling of E_g strongly depends on the composition and on the constituent material of core and shell because for this kind of geometry, at fixed diameter, the variation in the shape and localization of the wave function due to variation in composition are very relevant. It is important to point out that in our *core-shell* NWs, we cannot define a true type II band offset between Si and Ge, as presented by Yang *et al.*,[25] because the dimensions of the wires are too small; nevertheless, observing Fig. 9, we can recognize a certain tendency for valence states to be localized on Ge atoms and for conduction states to be localized on Si atoms.

V. CONCLUSIONS

We have presented first-principles investigation about SiGe NWs with different geometries and compositions; in particular, we have analyzed their FE, their electronic properties, and the nature of QCE pointing out their dependence from the wire diameter and from the composition of the system. The analysis of FE has shown that Ge_{core}/Si_{shell} NWs represent the most stable ones between the different SiGe heterostructures. This result confirms experimental outcomes, for which Ge_{core}/Si_{shell} NWs are the most common structures. We have obtained a complete characterization of the influence of the geometry and composition for the RQCE, showing how *abrupt* NWs present the most pronounced RCQE and a very easy way to predict and engine the energy band gap, which can have a strong relevance from a technological point of view. Moreover, we have explained, in particular, for *core-shell* NWs, the influence of composition on the variations in the wave-function localization.

ACKNOWLEDGMENTS

We acknowledge MIUR-PRIN 2007, MAE (Contributo Ministero Affari Esteri, Direzione Generale per la Promozione e la Cooperazione Culturale, Italia-Turchia), CINECA-CNR-INFM (for CPU time), and Ec e-13 ETSF project (INFRA Grant No. 211956); M.A. is grateful to David Kammerlander for useful discussions.

*stefano.ossicini@unimore.it

[1] D. D. D. Ma, C. S. Lee, F. C. K. Au, S. Y. Tong, and S. T. Lee, Science **299**, 1874 (2003).
[2] Y. Cui and C. M. Lieber, Science **291**, 851 (2001).
[3] A. M. Morales and C. M. Lieber, Science **279**, 208 (1998).
[4] S. E. Thompson and S. Parthasarathy, Mater. Today **9**, 20 (2006).
[5] J. Xiang, W. Lu, Y. Hu, Y. Wu, H. Yan, and C. M. Lieber, Nature (London) **441**, 489 (2006).
[6] B. Tian, X. Zheng, T. J. Kempa, Y. Fang, N. Yu, G. Yu, J. Huang, and C. M. Lieber, Nature (London) **449**, 885 (2007).
[7] W. Lu, J. Xiang, B. P. Timko, Y. Wu, and C. M. Lieber, Proc. Natl. Acad. Sci. U.S.A. **102**, 10046 (2005).
[8] L. Hu and G. Chen, Nano Lett. **7**, 3249 (2007).
[9] B. Tian, T. J. Kempa, and C. M. Lieber, Chem. Soc. Rev. **38**, 16 (2009).
[10] L. Tsakalakos, Mater. Sci. Eng., R. **62**, 175 (2008).
[11] G. Conibeer, M. Green, R. Corkish, Y. Cho, E.-C. Cho, C.-W. Jiang, T. Fangsuwannarak, E. Pink, Y. Huang, T. Puzzer, T. Trupke, B. Richards, A. Shalav, and K. Lin, Thin Solid Films **511**, 654 (2006).
[12] J. Yang, C. Jin, C. Kim, and M. Jo, Nano Lett. **6**, 2679 (2006).
[13] P. J. Pauzauskie and P. Yang, Mater. Today **9**, 36 (2006).
[14] A. I. Hochbaum, R. Chen, R. D. Delgado, W. Liang, E. C. Garnett, M. Najarian, A. Majumdar, and P. Yang, Nature (London) **451**, 163 (2008).
[15] J. Xiang, A. Vidan, M. Tinkham, R. M. Westervelt, and C. M. Lieber, Nat. Nanotechnol. **1**, 208 (2006).
[16] Y. Hu, H. O. Churchill, D. J. Reilly, J. Xiang, and C. M. Lieber, Nat. Nanotechnol. **2**, 622 (2007).
[17] L. Lauhon, M. S. Gudiksen, D. Wang, and C. M. Lieber, Nature (London) **420**, 57 (2002).
[18] W. W. Fang, N. Singh, L. K. Bera, H. S. Nguyen, S. C. Rustagi, G. Q. Lo, N. Balasubramanian, and D.-L. Kwong, IEEE Electron Device Lett. **28**, 211 (2007).
[19] N. Singh, K. D. Buddharaju, S. K. Manhas, A. Agarwal, S. C. Rustagi, G. Q. Lo, N. Balasubramanian, and D.-L. Kwong, IEEE Trans. Electron Devices **55**, 3107 (2008).
[20] N. D. Zakharov, P. Werner, G. Gerth, L. Shubert, L. Sokolov, and U. Gosele, J. Cryst. Growth **290**, 6 (2006).
[21] A. Nduwimana, R. Musin, A. Smith, and X. Wang, Nano Lett. **8**, 3341 (2008).
[22] D. B. Migas and V. E. Borisenko, Phys. Rev. B **76**, 035440 (2007).
[23] R. N. Musin and X. Q. Wang, Phys. Rev. B **74**, 165308 (2006).
[24] R. N. Musin and X.-Q. Wang, Phys. Rev. B **71**, 155318 (2005).
[25] L. Yang, R. N. Musin, X.-Q. Wang, and M. Y. Chou, Phys. Rev. B **77**, 195325 (2008).
[26] Q. Lu, K. Adu, H. R. Gutierrez, G. Chen, K. Lew, P. Nimmatoori, X. Xiang, E. C. Dickey, J. M. Redwing, and P. C. Eklund, J. Phys. Chem. C **112**, 3209 (2008).
[27] C. Nishimura, G. Imamura, M. Fujii, T. Kawashima, T. Saitoh, and S. Hayashi, Appl. Phys. Lett. **93**, 203101 (2008).
[28] S. P. Beckman, J. Han, and J. R. Chelikowsky, Phys. Rev. B **74**, 165314 (2006).
[29] M. Bruno, M. Palummo, A. Marini, R. Del Sole, and S. Ossicini, Phys. Rev. Lett. **98**, 036807 (2007).
[30] M. Bruno, M. Palummo, S. Ossicini, and R. Del Sole, Surf. Sci. **601**, 2707 (2007).
[31] M. Amato, M. Palummo, and S. Ossicini, Phys. Rev. B **79**, 201302(R) (2009).
[32] Y. Wu, Y. Cui, L. Huynh, C. J. Barrelet, D. C. Bell, and C. M. Lieber, Nano Lett. **4**, 433 (2004).
[33] E. L. de Oliveira, E. L. Albuquerque, J. S. de Sousa, and G. A. Farias, Microelectron. J. **40**, 762 (2009).
[34] This type of geometry is obtained by randomly substituting Si atoms with Ge ones; as in other theoretical studies (Ref. 33), to make our comparison with other geometries we refer only to one *random* configuration; this is not strong a approximation because taking into account another *random* configuration does not change qualitatively our results.
[35] K. Frey, J. C. Idrobo, M. L. Tiago, F. Reboredo, and S. Ogut, Phys. Rev. B **80**, 153411 (2009).
[36] L. Yang, J. Deslippe, C.-H. Park, M. L. Cohen, and S. G. Louie, Phys. Rev. Lett. **103**, 186802 (2009).
[37] M. Bruno, M. Palummo, A. Marini, R. Del Sole, V. Olevano, A. N. Kholod, and S. Ossicini, Phys. Rev. B **72**, 153310 (2005).
[38] It is well known that LDA underestimates energy band gap; nevertheless, it is important to highlight that it has been demonstrated that, for various types of nanostructures (Refs. 35–37), the self-energy corrections and the excitonic effects nearly cancel each other, making LDA conclusions about optical energy band gap still valid, in particular, for what concerns the scaling of the band gap with composition. Regarding the sole self-energy corrections, they strongly depend only on wires diameter. Since our analysis of the electronic gaps is done varying the concentration of Si or Ge at fixed NW size, our results remain valid apart from an almost rigid shift due the GW correction that depends only on the wire size.
[39] S. Baroni, A. Dal Corso, S. de Gironcoli, P. Giannozzi, C. Cavazzoni, G. Ballabio, S. Scandolo, G. Chiarotti, P. Focher, A. Pasquarello, K. Laasonen, A. Trave, R. Car, N. Marzari, and A. Kokaly (http://www.pwscf.org/).
[40] A. N. Kholod, V. L. Shaposhnikov, N. Sobolev, V. E. Borisenko, F. A. D'Avitaya, and S. Ossicini, Phys. Rev. B **70**, 035317 (2004).
[41] L. Vegard, Z. Phys. **5**, 17 (1921).
[42] S. J. Whang, S. J. Lee, W. F. Yang, and B. J. Cho, Appl. Phys. Lett. **91**, 072105 (2007).
[43] P. Logan and X. Peng, Phys. Rev. B **80**, 115322 (2009).
[44] Our choice regarding the use of the Vegard's law for the lattice parameter in the growth direction is supported by the very recent results presented of Logan and Peng (Ref. 43), which have shown that for NWs smaller than 2 nm, the variations in the relaxed lattice parameter in the direction of growth from the one constructed with bulk translational periodicity are very small (on the order of 0.01 Å) and that this strain causes variations smaller than 20 meV for the calculated electronic energy band gap. Moreover, in order to check if also for the SiGe NWs studied here, this is true, we have performed relaxations with a variable cell (that means a fully total-energy relaxation, not only of the atomic positions, but even of the cell parameters for x, y, and z directions); our results show how the deviations from the Vegard's law for *abrupt*, core-shell, and random SiGe NWs are on the order of 0.03 Å.
[45] S. B. Zhang and J. E. Northrup, Phys. Rev. Lett. **67**, 2339 (1991).
[46] E. Degoli, G. Cantele, E. Luppi, R. Magri, D. Ninno, O. Bisi, and S. Ossicini, Phys. Rev. B **69**, 155411 (2004).
[47] D. V. Melnikov and J. R. Chelikowsky, Phys. Rev. Lett. **92**,

046802 (2004).
[48] G. Cantele, E. Degoli, E. Luppi, R. Magri, D. Ninno, G. Iadonisi, and S. Ossicini, Phys. Rev. B **72**, 113303 (2005).
[49] L. E. Ramos, E. Degoli, G. Cantele, S. Ossicini, D. Ninno, J. Furthmüller, and F. Bechstedt, J. Phys.: Condens. Matter **19**, 466211 (2007).
[50] F. Iori, E. Degoli, M. Palummo, and S. Ossicini, Superlattices Microstruct. **44**, 337 (2008).
[51] R. Rurali and X. Cartoixà, Nano Lett. **9**, 975 (2009).
[52] S. Ciraci and I. P. Batra, Phys. Rev. Lett. **58**, 2114 (1987).
[53] S. Ciraci and I. P. Batra, Phys. Rev. B **38**, 1835 (1988).
[54] A. Ourmazd and J. C. Bean, Phys. Rev. Lett. **55**, 765 (1985).
[55] R. Ferrando, J. Jellinek, and R. L. Johnston, Chem. Rev. (Washington, D.C.) **108**, 845 (2008).
[56] C. L. Baley, A. Wander, S. Mukhopadhyay, B. G. Searle, and N. M. Harrison, Science and Technology Facilities Council, U.K., DL Technical Report No. DL-TR-2007–004, 2007 (unpublished).
[57] K. Romanyuk, J. Brona, and B. Voigtlander, Phys. Rev. Lett. **103**, 096101 (2009).
[58] As clearly explained by C. L. Baley *et al.* (Ref. 56), the thermodynamic stability can be described through the free Gibbs energy G, which is formally defined $G(T,P)=H(T,P)-TS(T,P)$: (5) where T is the temperature, S is the entropy, P is the pressure, and $H=\Phi^*-PV$ (V is the volume) is the formation enthalpy (FE) we have calculated, since we have assumed that the pressure is zero (the term $P\cdot V$ due to the change from the bulk to the nanowire is small and can be neglected). Clearly, at $T=0$ and $P=0$, the two quantities G and H coincide and, in the equation, the term containing the entropy S is canceled. So with our calculations, performed at temperature $T=0$, we cannot include the entropic contributes. It is worthwhile to note, however, that the approximation we used is physically valid at low temperatures, since, as recently showed by K. Romanyuk *et al.* (Ref. 57), in the case of SiGe systems, the effects of entropy are relevant only at high temperatures.
[59] L. E. Ramos, J. Furthmuller, and F. Bechstedt, Phys. Rev. B **72**, 045351 (2005).
[60] M. Stoffel, U. Denker, G. S. Kar, H. Sigg, and O. G. Schmidt, Appl. Phys. Lett. **83**, 2910 (2003).
[61] O. Kirfel, E. Mller, D. Grutzmacher, K. Kern, A. Hesse, J. Stangl, V. Holy, and G. Bauer, Appl. Surf. Sci. **224**, 139 (2004).
[62] A. V. Kolobov, H. Oynagi, K. Brunner, G. Abstreiter, Y. Maeda, A. A. Shklyaev, S. Yamasaki, M. Ichikawa, and K. Tanaka, J. Vac. Sci. Technol. A **20**, 1116 (2002).
[63] Y. Tu and J. Tersoff, Phys. Rev. Lett. **98**, 096103 (2007).
[64] J. Nah, E. S. Liu, D. Shahrjerdi, K. M. Varahramyan, S. K. Banerjee, and E. Tutuc, Appl. Phys. Lett. **94**, 063117 (2009).
[65] I. A. Goldthorpe, A. F. Marshall, and P. C. McIntyre, Nano Lett. **8**, 4081 (2008).
[66] Y. J. Hu, J. Xiang, G. C. Liang, H. Yan, and C. M. Lieber, Nano Lett. **8**, 925 (2008).
[67] D. Yao, G. Zhang, and B. Li, Nano Lett. **8**, 4557 (2008).
[68] All the E_g presented in the text are direct ones and are evaluated at the Γ point of the Brillouin zone.
[69] The diameters of the random SiGe NWs synthetized by Yang *et al.* range from 9 to 90 nm; but the effective diameters of nanowires studied are even smaller than the nominal diameters, due to the existence of significant oxide shells formed after growth. Our trend regarding the scaling of the energy band gap is in agreement with the results of Yang *et al.*, in particular, for the smallest SiGe wires synthetized.
[70] R. E. Bailey and S. Nie, J. Am. Chem. Soc. **125**, 7100 (2003).
[71] C. Bostedt, T. van Buuren, T. M. Willey, N. Franco, L. J. Terminello, C. Heske, and T. Möller, Appl. Phys. Lett. **84**, 4056 (2004).
[72] T. van Buuren, L. N. Dinh, L. L. Chase, W. J. Siekhaus, and L. J. Terminello, Phys. Rev. Lett. **80**, 3803 (1998).
[73] In Ref. 31, we have found, according to other experimental studies (Refs. 71 and 72), that, when we reduce the dimensionality of the material, the bulk E_g opens with a fixed ratio of the valence to the conduction band-edge shift $\frac{\Delta E_v}{\Delta E_c}$, which is nearly 1 for Si and nearly 2 for Ge NWs. We have noted that ΔE_v^{Si} is larger than ΔE_v^{Ge}, while ΔE_c^{Si} is smaller than ΔE_c^{Ge}. Moreover, it is important to point out that $|\Delta E_c^{\mathrm{Si}}-\Delta E_c^{\mathrm{Ge}}| \gg |\Delta E_v^{\mathrm{Si}}-\Delta E_v^{\mathrm{Ge}}|$.